VERIZONA PUBLISHER
Publishing Your Ideas

www.verizonaonlinepublishing.com
Vol: 1, Issue: 2

Journal of Nanoscience with Advanced Technology

Phase Field Simulation on the Effect of Interatomic Potentials at $L1_2$ Interface in $Ni_{75}Al_{16}Cr_9$ Alloy

Weiping Dong*[1], Zheng Chen[2]

[1] College of Engineering, Zhejiang Normal University (ZNU), Jinhua, 321004, PR China
[2] State Key Laboratory of Solidification Processing, School of Materials Science and Engineering, Northwestern Polytechnical University (NPU), Xi'an, 710072, PR China

***Corresponding author:** Weiping Dong, College of Engineering, Zhejiang Normal University, Jinhua, 321004, PR China; Tel: +86-18757606151; Email: dwp@zjnu.cn

Article Type: Research, **Submission Date**: 24 September 2015, **Accepted Date:** 12 October 2015, **Published Date:** 23 October 2015.

Citation: Weiping Dong, Zheng Chen (2015) Phase Field Simulation on the Effect of Interatomic Potentials at $L1_2$ Interface in $Ni_{75}Al_{16}Cr_9$ Alloy. J Nanosci Adv Tech 1(2): 30-34. doi: https://doi.org/10.24218/jnat.2015.09.

Abstract

Microscopic phase-field model with varying interatomic potentials was used to simulate the ordered domain interfaces formed between $L1_2$ phases in Ni-Al-Cr alloy. The behavior of interfaces migration and atoms segregation at the interfaces were investigated using the atomic evolution picture and occupation probability. The results show that there are stable domain interfaces and transition interface formed between $L1_2$ phases. The crystallization speed and the interfaces migration speed are related to the interatomic potentials. The crystallization speed gets faster when the interatomic potentials given 10% bigger than literature data, however, the crystallization speed gets slower and the final morphology of phases are very different while the interatomic potentials smaller. The elements of alloy have different preferences of segregation or depletion varying interatomic potentials at different interfaces (stable interfaces and migratory interfaces). In one case, at the interface of two Ni atoms between the planes (100) vs (100), the interface migration speed gets faster when the interatomic potentials bigger, and Al and Ni are depleted faster but Cr is segregated faster when the interatomic potentials given bigger values, conversely when the interatomic potentials given smaller values.

Keywords: Ni-Al-Cr alloy, Microscopic Phase-field method, Interatomic potential, Interface migration, Atoms segregation.

Introduction

There are two equilibrium phases $L1_2$ phase and $D0_{22}$ phase and two transient phases $L1_0$ phase and $L1_0$ (M=1) phase in Ni-Al-Cr high temperature superalloys [1-5]. Therefore, phase precipitation sequences exist during the early stage and the status of coexistence of multiple mixed phases is more likely to take place. During the mixed phases, there are many kinds of interfaces. It should be emphasized here that most materials processes are strongly affected by the interfacial properties during recrystallization and grain growth, especially in high temperature superalloys. Therefore, information on the interfaces is necessary to gain a better understanding. However, interfacial properties are hard to measure experimentally.

Many researchers have widely investigated the precipitation of Ni-Al-Cr alloys [6-10], but few on interfacial properties [11]. The difficulty in experimental works presents an opportunity for Microscopic Phase-field method simulations. The microscopic phase field method developed in the 1990s adopted in this study is a type of deterministic method which is capable of describing all diffusion processes including atomic clustering, ordering, crystal boundary migration, grown-up and coarsening of new phase, and formation of transient phase [12]. In addition, this method can reproduce microstructures, compositions and degree of order changes for the system in precipitation stage thoroughly. So it has shown a great advantage in the study of interfacial properties (interface migration and atoms segregation) during precipitation process. The Microscopic Phase-field method simulations have been successfully used for exploring interfacial properties, especially the kinds of interfaces in Ni-Al-V alloys [13-15]. The interatomic potentials are one of the basis input parameters of the Microscopic Phase-field method simulations, so it is quite reasonable to study the interfacial properties of Ni-Al-Cr alloys with the interatomic potentials. In this paper, the interface migration and atoms segregation of the ordered domain interfaces formed between $L1_2$ phases varying with the interatomic potentials will be simulated using the Microscopic phase-field method.

Microscopic Phase Field Model

The phase field dynamic equation is based on the Onsager and Ginzburg-Landau theories [16-19], which describes atomic configuration and the precipitation pattern of the ordered phases by the occupation probability $P(\vec{r},t)$ at the crystal lattice site $\vec{r}$ and the time *t*, whose change rate is proportional to the variation of free energy to it. For ternary system, atomic occupation probabilities is $P_A(\vec{r},t)+P_B(\vec{r},t)+P_C(\vec{r},t)=1$, where the subscripts *A*, *B* and *C* designate three kinds of atoms. In this simulation, it puts the simplification for crystalline defects, but just considers the integrated lattice to response atomic diffusion. The kinetic equation can be written as:

$$\begin{cases} \dfrac{dP_A(\vec{r},t)}{dt} = \dfrac{1}{k_B T}\sum_{r'}[L_{AA}(\vec{r}-\vec{r}')\dfrac{\partial F}{\partial P_A(\vec{r}',t)} \\ \qquad + L_{AB}(\vec{r}-\vec{r}')\dfrac{\partial F}{\partial P_B(\vec{r}',t)}] + \zeta_1(\vec{r},t) \\ \dfrac{dP_B(\vec{r},t)}{dt} = \dfrac{1}{k_B T}\sum_{r'}[L_{BB}(\vec{r}-\vec{r}')\dfrac{\partial F}{\partial P_B(\vec{r}',t)} \\ \qquad + L_{AB}(\vec{r}-\vec{r}')\dfrac{\partial F}{\partial P_A(\vec{r}',t)}] + \zeta_2(\vec{r},t) \end{cases} \quad (1)$$

In the mean-field approximation, the free energy for ternary system is given by:

$$\begin{aligned} F = & -\frac{1}{2}\sum_{r}\sum_{r'}[(-V_{AB}(\vec{r}-\vec{r}')+V_{BC}(\vec{r}-\vec{r}') \\ & + V_{AC}(\vec{r}-\vec{r}'))P_A(\vec{r})P_B(\vec{r}')+V_{AC}(\vec{r}-\vec{r}')P_A(\vec{r})P_A(\vec{r}') \\ & + V_{BC}(\vec{r}-\vec{r}')P_B(\vec{r})P_B(\vec{r}')] \\ & + k_B T\sum_{r'}[P_A(\vec{r})\ln(P_A(\vec{r}))+P_B(\vec{r})\ln(P_B(\vec{r})) \\ & + (1-P_A(\vec{r})-P_B(\vec{r}))\ln(1-P_A(\vec{r})-P_B(\vec{r}))] \end{aligned} \quad (2)$$

where the first sum represents the chemical energy, and the second sum represents the thermal dynamic energy of system, the $L(\vec{r}-\vec{r}')$ is a constant related to exchange probabilities of a pair of atoms at lattice sites r and r' per unit time, k_B is the Boltzmann constant. $V_{ab}(\vec{r}-\vec{r}')$ is the effective interactive energy given as:

$$V_{ab}(r-r') = W_a(r-r') + W_b(r-r') - 2W_{ab}(r-r') \quad (3)$$

where W_{aa}, W_{bb}, W_{ab} are pairwise potentials between a-a, b-b, and a-b. In order to keep reliability of simulations, the fourth nearest-neighbor interaction is adopted. Use V_{ab}^1, V_{ab}^2, V_{ab}^3, V_{ab}^4 to stand for the first-nearest, second-nearest, third-nearest and fourth-nearest interatomic potentials respectively. Then substitute them into the F.C.C., reciprocal space:

$$\begin{aligned} V_{ab}(\vec{k}) = & 4V_{ab}^1(\cos\pi h\cdot\cos\pi k + \cos\pi h\cdot\cos\pi l \\ & + \cos\pi k\cdot\cos\pi l) \\ & + 2V_{ab}^2(\cos 2\pi h + \cos 2\pi k + \cos 2\pi l) \\ & + 8V_{ab}^3(\cos 2\pi h\cdot\cos\pi k\cdot\cos\pi l + \cos\pi h \\ & \cdot\cos 2\pi k\cdot\cos\pi l + \cos\pi h\cdot\cos\pi k\cdot\cos 2\pi l \\ & + 4V_{ab}^4(\cos 2\pi h\cdot\cos 2\pi k + \cos 2\pi h\cdot\cos 2\pi l \\ & + \cos 2\pi k\cdot\cos 2\pi l) \end{aligned} \quad (4)$$

where *k*, *h* and, *l* are reciprocal lattice site through

$$\vec{k} = (k_x, k_y, k_z) = h\vec{a}_1^* + k\vec{a}_2^* + l\vec{a}_3^* \quad (5)$$

with $\vec{a}_1^*, \vec{a}_2^*, \vec{a}_3^*$ being the unit reciprocal lattice vectors of the F.C.C. structure.

It is convenient and even computationally advantageous to solve the kinetic equations in reciprocal space. First, the Euler method is used to solve the equation, and next the inverse Fourier transformation is carried out; finally the relationships between occupation probability and time are obtained.

Results and discussion

We use the microstructural evolution pictures to study the effect of interatomic potentials on the microstructure and interfaces migration. Under the conditions that temperature sets at 1100K, time steps t*= 300000 and 128*128 lattice points, using the references' interatomic potentials [1,20] (for Ni and Al interactions, $V^1_{Ni\text{-}Al}$=122.3, $V^2_{Ni\text{-}Al}$=6.0, $V^3_{Ni\text{-}Al}$=16.58, $V^4_{Ni\text{-}Al}$=-6.82; for Ni and Cr interactions, $V^1_{Ni\text{-}Cr}$=-84.8, $V^2_{Ni\text{-}Cr}$=46.8, $V^3_{Ni\text{-}Cr}$=10.4, $V^4_{Ni\text{-}Cr}$=-33.2; and for Al and Cr interactions, $V^1_{Al\text{-}Cr}$=-140.0, $V^2_{Al\text{-}Cr}$=-40.0, $V^3_{Al\text{-}Cr}$=74.5, $V^4_{Al\text{-}Cr}$=0.0 (unit: meV)) or 10% smaller than that or 10% higher than that, Figure 1 demonstrates microstructural evolution pictures of $Ni_{75}Al_{16}Cr_9$ alloy with varying time steps. The time step Δt is 0.0002, and the thermal fluctuations are removed after nucleation, the system chooses the dynamic path automatically. In this paper, we focus on the first-nearest interatomic potentials which usually known as the biggest and the most impact of all the interatomic potentials. V_{ab}^1 interatomic potentials of Ni-Al, Ni-Cr and Al-Cr are used in Figure1(a2-d2) as 122.3 meV, -84.8 meV and -140 meV, respectively. With the same values in other parameters, V_{ab}^1 interatomic potentials are changed in Figure 1(a1-d1) as 10% smaller and Figure 1(a3-d3) as 10% bigger, respectively.

From Figure 1(a1)-(a3), it demonstrates that the V_{ab}^1 interatomic potentials have great effect on microstructure at the early stage of precipitation at time step 3000. The map is totally blue which indicates the basal body is in complete disorder as shown in Figure 1(a1) while $L1_2$ phases precipitated in Figure 1(a2) and (a3). In other words, the crystallization beginning speed gets slower when the interatomic potentials given 10% smaller than literature data according to the Figure 1(a1) and (a2); and the crystallization beginning speed gets faster while the interatomic potentials given bigger values as in Figure 1(a2) and (a3). As time goes by, $L1_2$ phase precipitated gradually. We can see the V_{ab}^1 interatomic potentials don't have much effect on the intermediate state microstructure during the time steps of 6000 to 18000 seen in the Figure 1(b1)-(c3), except the Figure 1(c1) in which the phase microstructure is different from Figure 1(c2) and (c3) as ellipse marked. The arrangement and volume of phase microstructure in evolutional morphology are very different as marked in Figure (d1)-(d3), which testifies to the fact that the final morphology of phases and the interfaces migration speed are greatly affected by the interatomic potentials. The morphology of phases depends on the interfaces migration as known in literature [13-15]. The results in Figure (d1)-(d3) show that there are stable domain interfaces and transition interfaces formed between $L1_2$ phases. The interfaces ellipse marked migrate very differently while rectangle marked migrate just a little bit. The migration ability of interface is related to its structure while the migration speed is related to the interatomic potentials.

More generally, interatomic potentials have great influence on crystallization speed, the phase microstructure, the interfaces and their migration speed which determine the properties of alloys.

To study the effect of interatomic potentials on the solute segregation and depletion of interfaces, the concentration distributions of alloy elements of two Ni atom between the planes (100) vs (100) shown in Figure 1(d1-D), represented by the average site occupation probabilities of alloy elements varying interatomic potentials, along the lattice site across the interfaces were calculated as in Figure 2. The elements of alloy have different preferences of segregation or depletion varying interatomic potentials at different interfaces (stable interfaces

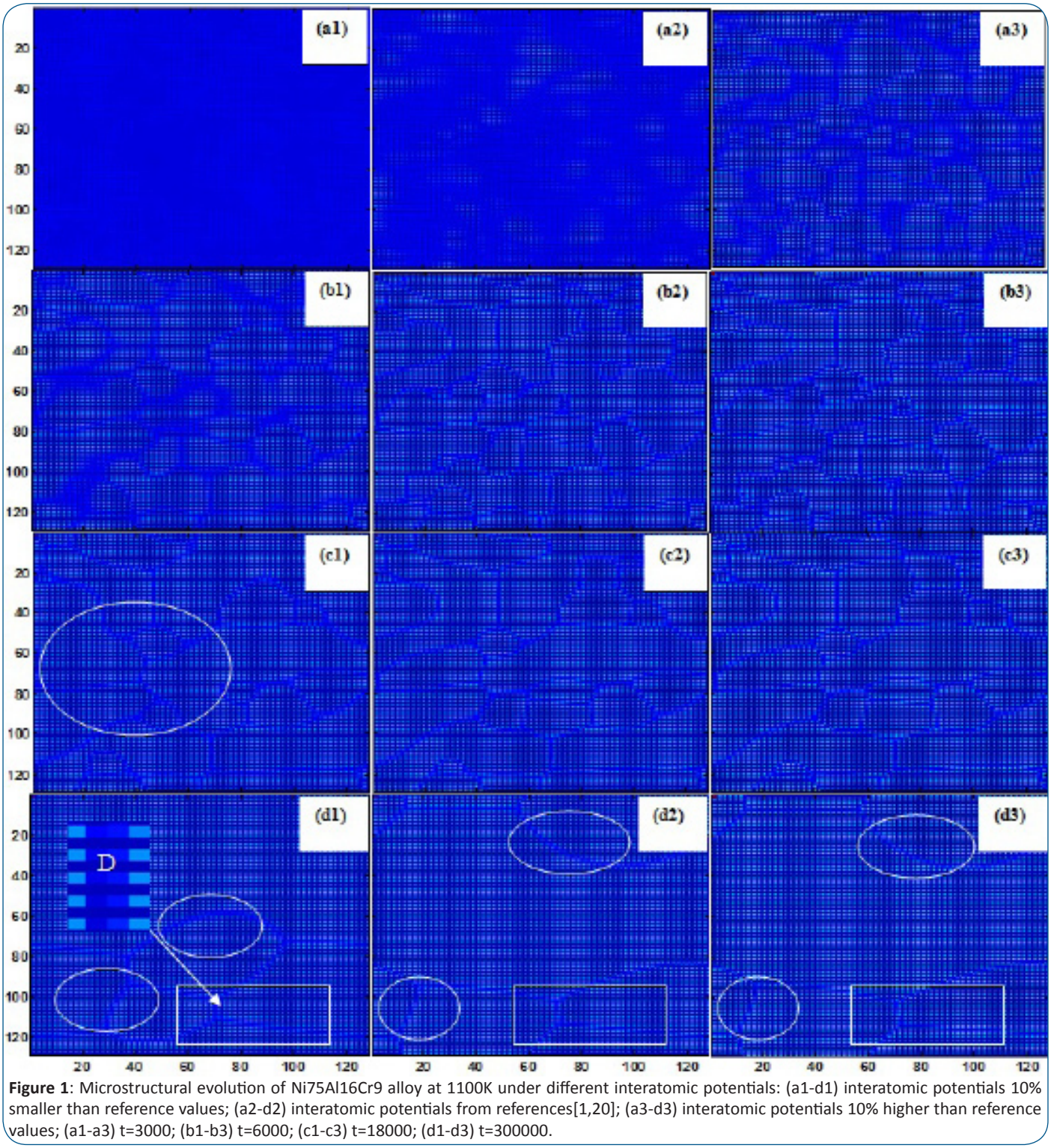

Figure 1: Microstructural evolution of Ni75Al16Cr9 alloy at 1100K under different interatomic potentials: (a1-d1) interatomic potentials 10% smaller than reference values; (a2-d2) interatomic potentials from references[1,20]; (a3-d3) interatomic potentials 10% higher than reference values; (a1-a3) t=3000; (b1-b3) t=6000; (c1-c3) t=18000; (d1-d3) t=300000.

and migratory interfaces) similarly to references results [13-15]. From all the curves, we can see the compositions of alloy elements at the interfaces are different from that inside the domains and Ni and Al deplete but V segregates. The migratory interface forms between this $L1_2$ phases planes (100) vs (100) and migrates from the lattice site 67-69 to 69-71 or 71-73.

From Figure 2(a), the concentration curves across the interfaces of Ni and Al are lower and the composition of Cr is raised when the V_{ab}^{1} interatomic potentials given 10% bigger than literature data at 3000 step, which indicates Ni and Al depleted but Cr segregated and the interface forms agreeing with Figure 1(a3) and l. The degrees of segregation and depletion of alloy elements are different when given the different interatomic potentials at 6000 step in Figure 2(b). The concentration curves across the interface of Ni and Al are the lowest when given 10% bigger potentials and the Cr is the highest, which means Al and Ni are depleted faster but Cr is segregated faster when the interatomic potentials given bigger values, Whereas the opposite. Analyzing the Figure 2(c), the interface when given 10% smaller potentials migrates from the lattice site 67-69 to 69-71 while the interface when given bigger potentials migrates from the lattice site 67-69 to 71-73, which demonstrates the interface migration speed gets faster when given the bigger interatomic potentials.

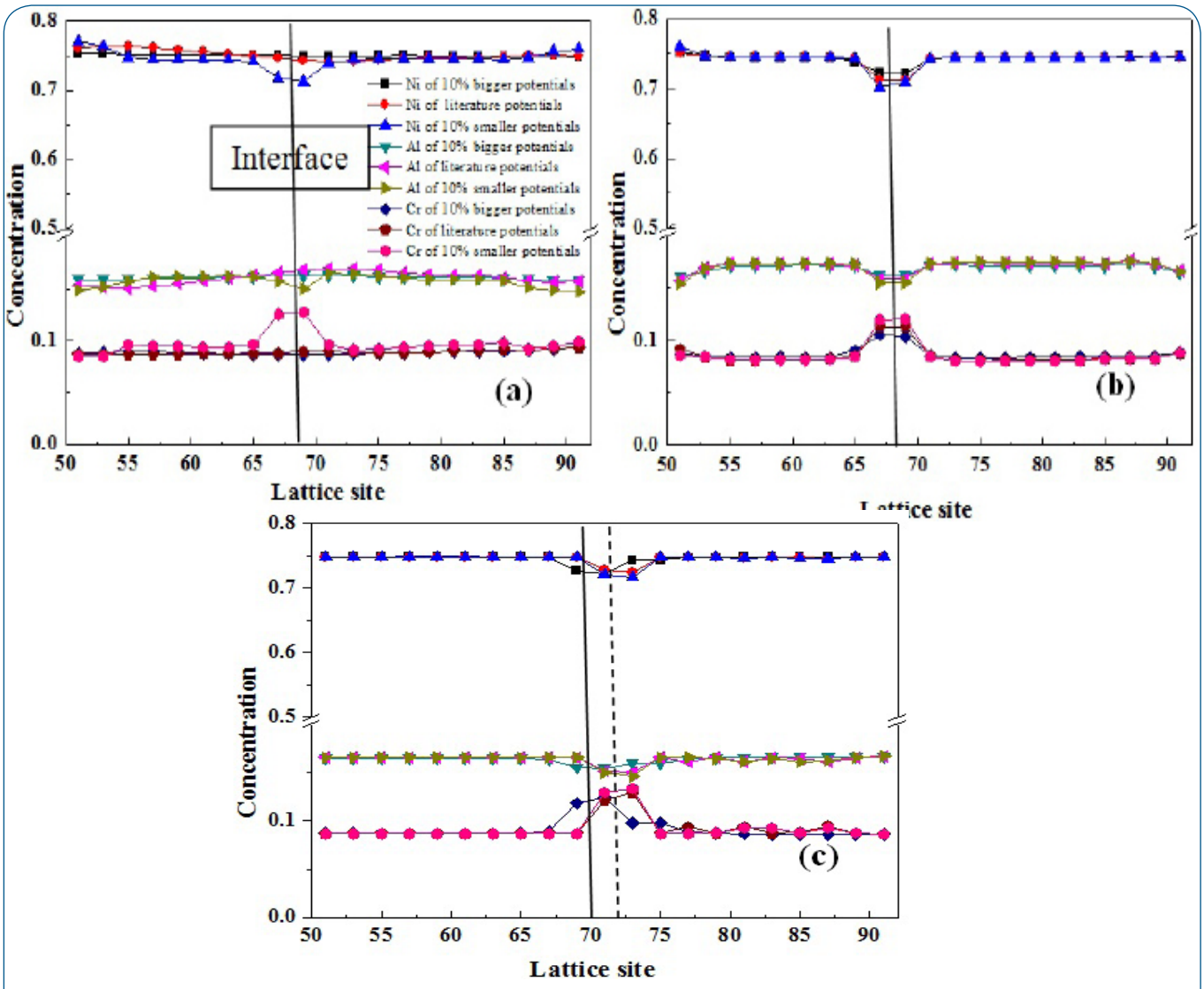

Figure 2: Concentration distributions of alloying elements varying interatomic potentials along the lattice site across interfaces (Fig.1 d1-D) for different time steps: (a) t=3000; (b) t=6000; (c) t=300000.

Conclusions

1) The results show that the interatomic potentials has great influence on the crystallization, the phase microstructure, the interfaces structure, segregation or depletion at the interfaces and their migration.

2) It is presented that the interatomic potentials affect the early stage of precipitation. The microstructure is disorder and the crystallization beginning speed gets slower when the interatomic potentials given 10% smaller than literature data. However, the $L1_2$ phases completely formed and the crystallization speed get faster when given bigger potentials. And the final morphology of phases are also very different varying with the potentials.

3) The results indicate that the alloy elements segregation or depletion varying interatomic potentials at different interfaces. In case of two Ni atoms between the planes (100) vs (100), Al and Ni are depleted faster but Cr is segregated faster when the interatomic potentials given bigger values, whereas the opposite. And moreover the (100) vs (100) interface migration speed gets faster when given bigger potentials.

Acknowledgements

This work is supported by the Zhejiang Provincial Natural Science Foundation of China (LQ14E010002) and the National Natural Science Foundation of China (51501165).

References

1. Pareige C, Soisson F, Martin G, Blavettea D. Ording and phase separation in Ni-Cr-Al: Monte Carlo simulations vs three-dimensional atom probe. Acta Mater. 1999; 47(6):1889-1899. doi:10.1016/S1359-6454(99)00054-3.

2. Lu YL, Chen Z, Li YS, Wang YX. Microscopic Phase-field simulation coupled with elastic strain energy for precipitation process of Ni-Cr-Al alloys with low Al content. Trans. Nonferrous Met. Soc. China. 2007; 17(1):64-71. doi:10.1016/S1003-6326(07)60049-1.

3. Zhang JX, Chen Z, Lai QB, Zhao Yan, Wang Yongxin. Microscopic Phase-field simulation of Re-ageing temperature on precipitation of Ni-Cr-Al alloys. Chinese J. Aeronaut. 2009; 22(5):551-557. doi:10.1016/S1000-9361(08)60140-5.

4. Dong WP, Chen Z, Wang YX. Energy studies of precipitation sequence in $Ni_{75}Al_{10}Cr_{15}$ alloy based on the phase field theory. Sci. China Phys. Mech. 2011; 54(5):821-826. doi: 10.1007/s11433-011-4306-0.

5. Lu YL, Chen Z, Li X, Tang K. Microscopic phase-field study of the effect of temperature on the pre-precipitates of Ni-Al-Cr alloy. Comp. Mater. Sci. 2015; 99:247-252. doi:10.1016/j.commatsci.2014.11.042.

6. Lu YL, Jia DW, Hu TT, Chen Z, Zhang Li. Phase-field study the effects of elastic strain energy on the occupation probability of Cr atom in Ni-Al-Cr alloy. Superlattice. Microst. 2014; 66:105-111. doi:10.1016/j.spmi.2013.11.025.

7. Nguyen HVP, Song SA, Seo DH, Park DN, Ham HC, Oh IH, et al. Fabrication of Ni-Al-Cr alloy anode for molten carbonate fuel cells. Mater. Chem. Phys. 2012; 136(2-3):910-916. doi:10.1016/j.matchemphys.2012.08.018.

8. Lu YL, Chen Z, Wang YX, Zhang J, Yang K. Phase-field study the effect of elastic strain energy on the incubation period of Ni-Cr-Al alloys. Comp. Mater. Sci. 2011; 50(6):1925-1931. doi:10.1016/j.commatsci.2011.01.042.

9. Mao ZG, Christopher BM, Sudbrack CK, Martina G, Seidmana DN. Kinetic pathways for phase separation: An atomic-scale study in Ni-Al-Cr alloys. Acta Mater. 2012; 60(4):1871-1888. doi:10.1016/j.actamat.2011.10.046.

10. Mignanelli PM, Jones NG, Hardy MC, Stone HJ. The influence of Al: Nb ratio on the microstructure and mechanical response of quaternary Ni-Cr-Al-Nb alloys. Mater. Sci. Eng. A. 2014; 612:179-186. doi:10.1016/j.msea.2014.06.021.

11. Li X, Zhang XN, Liu CP, Wang CY, Yu T, Zhang Z. Regular γ/γ' phase interface instability in a binary model nickel-based single-crystal alloy. J. Alloy. Compd. 2015; 633:366-369. doi:10.1016/j.jallcom.2015.01.109.

12. Raable D. Coputational Materials Science. Beijing: Chemistry Industry; 2002. 10 p.

13. Zhang MY, Chen Z, Wang YX, Lu YL, Zhang LP, Zhao Y. Microscopic phase-field simulation of ordered domain interfaces formed between DO_{22} phases along [100] direction. Trans. Nonferrous Met. Soc. China. 2009; 19(3):686-693. doi:10.1016/S1003-6326(08)60334-9.

14. Zhang MY, Wang YX, Chen Z, Jing Z, Yanli L, Weiping D. Microscopic Phase-Field Study on the Atomic Structure and Migration Characteristic of Ordered Domain Interfaces. Rare Metal Mater. Engin. 2010; 39(7):1147-1151. doi: 10.1016/S1875-5372(10)60110-5.

15. Zhang MY, Chen Z, Wang YX, Guang MA, Lu YL, Fan XL. Effect of atomic structure on migration characteristic and solute segregation of ordered domain interfaces formed in $Ni_{75}Al_xV_{25-x}$. Trans. Nonferrous Met. Soc. China. 2011; 21(3):604-611. doi:10.1016/S1003-6326(11)60757-7.

16. Khachaturyan AG. Theory of Structural Transformation in Solids. New York: Wiley; 2008. 129 p.

17. Chen LQ, Khachaturyan AG. Computer Simulation of Structural Transformations During Precipitation of an Ordered Intermetallic Phase. Acta Metall. Mater. 1991; 39(11):2533-2551. doi:10.1016/0956-7151(91)90069-D.

18. Wang Y, Chen LQ, Khachaturyan AG. Kinetics of the Strain-Induced Morphological Transformation in Cubic Alloys with Miscibility Gap. Acta Metall. Mater. 1993; 41(1):279-296. doi:10.1016/0956-7151(93)90359-Z.

19. Poduri R, Chen LQ. Computer simulation of the kinetics of order-disorder and phase separation during precipitation of δ'(Al_3Li) in Al-Li alloys. Acta Mater. 1998; 45(1):1719-1729. doi:10.1016/S1359-6454(96)00137-1.

20. Poduri R, Chen LQ. Computer simulation of atomic ordering and compositional clustering in the pseudobinary Ni_3Al-Ni_3V system. Acta Mater. 1998; 46(5):1791-1729. doi:10.1016/S1359-6454(97)00335-2.